European Journal of Pharmaceutics and Biopharmaceutics 75 (2010) 16–25

Contents lists available at ScienceDirect

European Journal of Pharmaceutics and Biopharmaceutics

journal homepage: www.elsevier.com/locate/ejpb

Research paper

A critical evaluation of self-interaction chromatography as a predictive tool for the assessment of protein–protein interactions in protein formulation development: A case study of a therapeutic monoclonal antibody

Virginie Le Brun [a], Wolfgang Friess [a], Stefan Bassarab [b], Silke Mühlau [b], Patrick Garidel [b,*]

[a] Department of Pharmacy, Pharmaceutical Technology and Biopharmaceutics, Ludwig-Maximilians-Universität München, Germany
[b] Department Process Science/Biopharmaceuticals, Pharmaceutical Development, Boehringer Ingelheim Pharma GmbH & Co. KG, Biberach an der Riss, Germany

ARTICLE INFO

Article history:
Received 13 May 2009
Accepted in revised form 20 January 2010
Available online 25 January 2010

Keywords:
Immunoglobulin
Antibody
Self-interaction chromatography
Osmotic second virial coefficient
B_{22}
Colloidal stability
Protein interactions

ABSTRACT

The aim of this study was to establish and evaluate a screening method for the physical characterization of protein–protein interactions of therapeutic proteins based on the determination of the osmotic second virial coefficient (B_{22}). B_{22} of an IgG1 was measured by self-interaction chromatography (SIC) and was compared to data obtained from static light scattering (SLS). As assessed by Fourier transform infrared spectroscopy (FTIR), the protein coupling to chromatography particles had no relevant influence on the three-dimensional native structure of the IgG1.

B_{22} variations could be measured for physiological relevant excipient concentrations. Significant positive B_{22} values were observed for the following solution conditions of the investigated antibody: (i) acidic pH conditions, (ii) low buffer concentrations, (iii) low salt concentrations and (iv) high amino acid concentrations. B_{22} was compared to IgG1 stability data derived from a study conducted for 12 weeks at 40 °C. A concentration of 5 mM histidine, which was the most promising buffer candidate according to B_{22}, showed a slightly better physical stability (as assessed by turbidity and size exclusion chromatography) compared to the other tested formulations. This is confirmed in a stress study investigating the colloidal stability.

Thus, measuring protein–protein interactions with SIC appeared as a promising screening tool for physical characterization of protein formulations for cases in which the protein stability is governed by interparticle interactions.

© 2010 Elsevier B.V. All rights reserved.

1. Introduction

As proteins have poor bioavailability by most application routes, protein drugs are usually administered intravenously favoring an excellent control during clinical administration [1,2]. Antibodies play a major role in the treatment of many diseases such as cancer, infectious diseases, allergy, autoimmune diseases and inflammation. In numerous cases, monoclonal antibodies have to be administered frequently and at high doses (up to a few hundreds mg per application). To improve patient compliance, subcutaneous dosage forms are favored leading to the need of a small injection volume with a high protein concentration. Consequently, high concentrated protein formulations (up to 150 mg/ml) with good protein stability are required [3]. Reaching high concentrated protein formulations requires the control of chemical and physical stabilities. The main physical instability lies in protein aggregation that can be prevented by two main mechanisms. The first one consists of increasing the thermodynamic stability of the protein native state, shifting the equilibrium toward the folded protein state and reducing the concentration of unfolded states, the latter being more prone to protein aggregation [1]. The second route is based on improving the protein's colloidal stability by reducing attractive protein–protein interactions [3]. Beyond this, it is also possible to design the protein framework such to avoid hot spots prone to the formation of aggregates [4–7].

Protein structural changes of high concentration protein solutions were directly characterized by differential scanning calorimetry (DSC) [8], front surface fluorescence spectroscopy [8], circular dichroism (CD) [8] and Fourier transform infrared spectroscopy (FTIR) [8,9], whereas protein interactions were studied by static light scattering (SLS) [10], isothermal titration calorimetry (ITC) [10], ultrasonic storage modulus [11] or sedimentation equilibrium and osmotic pressure [12]. Besides the aforementioned techniques for the analysis of protein interactions, the strength and the range of protein colloidal interactions can also be evaluated by the osmo-

* Corresponding author. Department Process Science/Biopharmaceuticals, Pharmaceutical Development, Boehringer Ingelheim Pharma GmbH & Co. KG, D-88397 Biberach an der Riss, Germany. Tel.: +49 7351545556; fax: +49 7351835556.
E-mail address: Patrick.Garidel@boehringer-ingelheim.com (P. Garidel).

0939-6411/$ - see front matter © 2010 Elsevier B.V. All rights reserved.
doi:10.1016/j.ejpb.2010.01.009

tic second virial coefficient (B_{22}), which measures the non-ideal solution behavior arising from two body interactions. As B_{22} of diluted protein solutions has been shown to correlate with B_{22} of concentrated protein solutions [13], B_{22} measurements may be realized under diluted conditions and be representative of concentrated protein solutions.

Different techniques were used for the investigation of protein–protein interactions and protein self-association [14–18]. However, most of them are not adapted to high throughput screening [19–21]. Various chromatography-based techniques have emerged in the last years in order to characterize protein–protein interactions [22–29] more rapidly, especially the studies presented by Lenhoff, Przybycien and other colleagues showed the potential of chromatography-based assays [30–32].

In the presented study, the determination of the strength of antibody–antibody interactions via B_{22} is used for the identification of solution conditions minimizing protein aggregation. However, the majority of the published studies were performed with model proteins such as lysozyme using SLS methods [33–35] or self-interaction chromatography (SIC) [32,36–38]. Only few data of therapeutic relevant proteins are available. SIC was recently used to establish the crystallization conditions of a monoclonal antibody [39]. By correlating phase diagrams with B_{22} data, Ahamed et al. [39] provided useful information not only for a fundamental understanding of the phase behavior of monoclonal antibodies, but also for understanding the reason why certain proteins are extremely difficult to crystallize.

Liu et al. have determined B_{22} of different monoclonal antibodies by sedimentation equilibrium to determine the reversible protein self-association mediated by electrostatic interactions [40]. The effect of buffer on the stability of interferon-tau (IFN-tau) was compared to B_{22} (determined by SIC) [41] indicating that histidine buffer, which gave the best stabilization of IFN-tau during thermal stress, had a minor effect on the colloidal stabilization of IFN-tau, as the buffer species had little effect on B_{22}. Thus, this example shows that B_{22} correlates with colloidal stability. The study of an IgG2 showed that the B_{22} analysis based on light scattering was consistent with rheology studies [11,42], but no correlation was found between B_{22} and long-term aggregation as the transition to the IgG2 unfolded state was first responsible for protein aggregation. It is important to keep in mind, that B_{22} only considers the interactions between native protein molecules, and that the interactions between native and unfolded or partially unfolded proteins are not represented in the B_{22} term. Thus, B_{22} is not a predictive parameter for aggregation via a pathway including structural changes.

Similarly, the stability of recombinant human granulocyte colony-stimulating factor (rh-GCSF) was compared to the free energy of protein unfolding and B_{22} measured by SLS (static light scattering). Obviously, no correlation between B_{22} and protein stability could be established given that the rh-GCSF aggregation first involved perturbation of its native structure [43]. Lastly, Alford et al. measured the attraction forces between monomer–monomer (B_{22}), monomer–dimer (B_{23}) and dimer–dimer (B_{33}) of recombinant human interleukin-1 receptor antagonist (rhIL-1ra) by membrane osmometry and SLS to differentiate the contribution of the different protein species [10,44] and showed that only the interactions between monomer–dimer were attractive. They observed with increasing rhIL-1ra concentration dimerisation is favored which is enthalpically driven. In solution rhIL-1ra exists as a monomer–dimer equilibrium. By incubation of 100 mg/ml rhIL-1ra solutions at 37 °C, the attractive monomer–dimer interactions led to the formation of a trimer form, which was the rate-limiting step in rhIL-1ra aggregation.

Overall, B_{22} was a poor predictive tool of protein stability in those previous examples, since the colloidal stability was not the rate-limiting step of protein aggregation. Aggregation was induced by changes in the protein structure, which is not considered in the B_{22} theory and application. However, it was shown by a number of studies that B_{22} correlated with protein solubility, which is an important parameter for protein colloidal stability [45–51].

This work is focused on the application of SIC for a monoclonal antibody type IgG1. First, it was investigated whether coupling of the antibody to the chromatography particle may affect the structure of the antibody. Subsequently, the influence of the different solution conditions was tested with regard to interactions between the IgG1 molecules: (a) protonation degree of IgG1 (pH), (b) buffer species and their concentration, (c) NaCl concentration and (d) the presence of amino acids. Finally, B_{22} was compared to IgG1 stability to evaluate its potential impact as a screening tool for protein formulations.

2. Materials and methods

2.1. Materials

A humanized monoclonal IgG1 antibody, which was formulated at a concentration of 5 mg/ml in phosphate buffered saline at pH 6.2, was provided by Boehringer Ingelheim Pharma GmbH & Co. KG (Biberach, Germany). Toyoperal AF Formyl 650 M was obtained from Tosoh Bioscience (Stuttgart, Germany). Sodium acetate, sodium chloride, sodium citrate, sodium cyanoborohydride, L-arginine monohydrochloride, L-histidine and L-methionine were purchased from Merck (Darmstadt, Germany), ethanolamine form Prolabo (Fontenay sous bois, France), sodium phosphate from Riedel-de Haën (Seelze, Germany), sodium succinate from Alfa Aesar (Karlsruhe, Germany), glycine and ethylenediaminetetraacetic acid (EDTA) from Sigma Aldrich (Steinheim, Germany) and bicinchoninic acid (BCA) protein assay kit from Novagen (Madison, WI, USA).

The pH of the solutions was adjusted using hydrochloric acid or sodium hydroxide and measured with a pH meter Inolab level 1 from WTW (Weilheim, Germany). The protein concentrations were evaluated photometrically with an Agilent 8453 instrument (Agilent Technologies, Waldbronn, Germany) at 280 nm using as extinction coefficient 1.44 ml mg^{-1} cm^{-1}.

2.2. Methods

2.2.1. IgG1 immobilization

Three-milliliter Toyopearl AF Formyl 650 M particles were washed on a glass frit with 0.2 μm hydrophilic polyethersulfone membrane filter with first 250 ml de-ionized water and secondly 50 ml of 0.1 M potassium phosphate buffer pH 7.5. The washed particles were recovered and mixed with 10 ml IgG1 solution (5.0 mg/ml in 0.1 M potassium phosphate buffer pH 7.5) and 90 mg sodium cyanoborohydride were added as activator of protein binding. The suspension was mixed over night on a rotary mixer. At the end of the coupling reaction, the particles were first washed with 200 ml of 0.1 M potassium phosphate buffer to remove unbound protein and then added to 15 ml of 1 M ethanolamine pH 8.0 and 20 mg sodium cyanoborohydride to cap the remaining active groups of the matrix. The suspension was incubated on a rotary mixer for 4 h. At the end of the reaction, the particles were washed with 200 ml of 1 M sodium chloride solution pH 7.0. The amount of bound IgG1 was determined both by analyzing the difference between the absorbance of the initial protein solution and the wash solutions (A280) and in addition by determining the immobilized protein quantity directly by BCA protein assay. Loadings ranged from 11 to 17 mg IgG1/g resin.

The chromatography particles were suspended as a 50%-slurry in 1 M NaCl and composed of a 50 mM sodium phosphate solution

pH 6.0. Approximately 2.5 ml slurry was packed in a Tricorn® 5/50 column (GE Healthcare, Uppsala, Sweden) with the same buffer at 3 ml/min flow rate during 15 min using a FPLC system (Äkta Purifier, GE Healthcare, Uppsala, Sweden). At the end of the packing procedure, the flow rate was maintained to 0.75 ml/min for at least 1 h. Columns were stored at 4 °C in a 5 mM sodium phosphate solution pH 7.0 containing 0.05% sodium azide and remained stable at least 8 weeks.

2.2.2. ATR–FTIR investigation and second derivates

FTIR-spectroscopy measurements were conducted with a Tensor 37 spectrometer (Bruker Optics, Ettlingen, Germany) as described previously [9]. Filtered samples were dried overnight at room temperature and measured by the attenuated total reflection (ATR) technique with the MVP unit at 20 °C. Each sample measurement was the average of 120 scans and was measured 3 times. The spectra were collected from 4000 to 1000 cm^{-1} with a 4 cm^{-1} resolution. The particle spectrum was manually subtracted from the bound protein particle spectrum, and the protein spectra were further processed by vector normalization on the amide I band [9,52].

2.2.3. Determination of the osmotic second virial coefficient B_{22}

B_{22} measurements were realized with a FPLC Äkta Purifier system equipped with a UV detector (A280) and an auto-sampler. Before each run, the column was equilibrated with 10 ml of the protein-free mobile phase. The column dead volume was estimated by injection of a 1% acetone solution. All experiments were carried at 25 °C and at a flow rate of 0.3 ml/min. 0.1 mg of IgG1 was injected. Each sample was measured 3 times.

Chromatogram peaks were analyzed with the UNICORN® software (GE Healthcare, Uppsala, Sweden). The retention volume was determined at the peak maximum. The retention measurements were used to calculate the retention factor k' (Eq. (1)):

$$k' = \frac{V_o - V_r}{V_o} \quad (1)$$

where V_r is the volume required to elute the protein in the mobile phase and V_0 the retention volume of non-interacting species (e.g. acetone). B_{22} is related to the retention factor as follow [37]:

$$B_{22} = B_{HS} - \frac{k'}{\rho_s \Phi} \quad (2)$$

$$B_{HS} = \frac{16}{3}\pi^3 \frac{N_A}{M_2^2} \quad (3)$$

where ρ_s is the number of immobilized molecules per unit area, Φ the phase ratio, which is the total surface available to the mobile phase protein, r the protein radius, N_A the Avogadro's number and M_2 the protein (index 2) molecular weight. For more details see [37,53,54].

Selected SIC results were compared to SLS measurements. B_{22} as derived from SLS was measured according to the methods described by Valente et al. [55] and Velev et al. [56]. The scattered light intensity of a protein formulation was measured as a function of protein concentration in the concentration range of 1–15 mg/ml with 5 protein concentrations investigated per formulation, and the data were evaluated according to the Kratochvil method.

2.2.4. Determination of the IgG1 net charge

The IgG1 molecule net charge was calculated with the EMBOSS software [57].

2.2.5. Turbidity

Turbidity was measured as photometric absorbance at 350 nm against WFI as blank value in triplicate with a Fluostar Omega microplate reader (BMG Labtech, Offenburg, Germany). The reference suspensions described in the European Pharmacopoeia present the following absorbance at 350 nm [58]: Ref. I < 17 ± 2 mAbs, Ref. II < 32 ± 3 mAbs, Ref. III < 85 ± 1 mAbs and Ref. IV < 144 ± 5 mAbs.

2.2.6. Size exclusion high-performance liquid chromatography (SE-HPLC)

SE-HPLC was used to determine the amount of soluble protein aggregates in the IgG1 solutions. The measurements were performed on a HP 1100 instrument (Agilent Technologies, Waldbronn, Germany) in connection with a SWXL guard column and a TSK3000SWXL column (Tosoh Bioscience, Stuttgart, Germany). The mobile phase consisted of 0.05 M sodium-dihydrogen phosphate dihydrate and 0.6 M sodium chloride and was adjusted to pH 7.0 with NaOH 2 N. The flow rate was 0.5 ml/min, the injection volume 10 µl and the UV signal was detected at 280 nm.

2.2.7. Microcalorimetry

The thermograms of 2 mg/ml IgG1 solutions were determined in triplicate by using a Differential Scanning Calorimeter of VP-DSC type (Microcal, Northampton, USA) at a scan rate of 1 K/min. Thermograms were obtained after subtraction of the corresponding buffer scan.

2.2.8. Stirring stress

Stirring stress at room temperature was performed using 10R glass vials (Schott, Mainz, Germany) filled with 5 ml of 20 mg/ml IgG1 solution according to the stirring protocol recently described [59]. At defined time points, a vial was removed and analyzed for protein aggregation by turbidity.

3. Results and discussion

3.1. IgG1 characterization after binding on chromatography particles

The SIC method consists of the immobilization of the studied protein on chromatography particles and of the injection of the same initial protein, in various solution conditions, to measure free native protein – immobilized native protein interactions. IgG1 primary amine groups are coupled to the aldehyde-bearing Toyopearl AF Formyl 650 chromatography particles under mild conditions, resulting in the formation of stable secondary amine linkage between IgG1 and the resin. FTIR-spectroscopy was used to analyze the protein's secondary structure, in order to analyze the influence of coupling upon binding. The protein secondary structure is related to a certain band structure of the amide I and II vibration [9,52]. The overall amide I band is the sum of sub-bands, which are assigned to the different secondary structure elements like alpha-helix, beta-sheet, turn or random coil. These structural elements can be determined, depending on the used data base and software, with a precision of ± 2%.

Fig. 1A–D shows the spectral region from 1600–1700 cm^{-1} representing the amide I band for the native antibody in solution (Fig. 1A) and under various conditions. The second derivative spectrum of the amide I band is included in the figure. The amide I band of the native antibody in solution is characterized by three sub-bands located at 1614, 1639 and 1690 cm^{-1} which are typical for IgGs having predominantly β-sheet secondary structure elements [60–62]. IgG1 bound to Toyopearl particles (Fig. 1C) was characterized by a main band at 1640 cm^{-1} and two small bands at 1687 and 1611 cm^{-1}. Although the overall band shape is slightly altered, no major structural change could be detected due to the protein binding process. Thus, the protein secondary structure is mainly retained after coupling of the antibody to the chromatography particles.

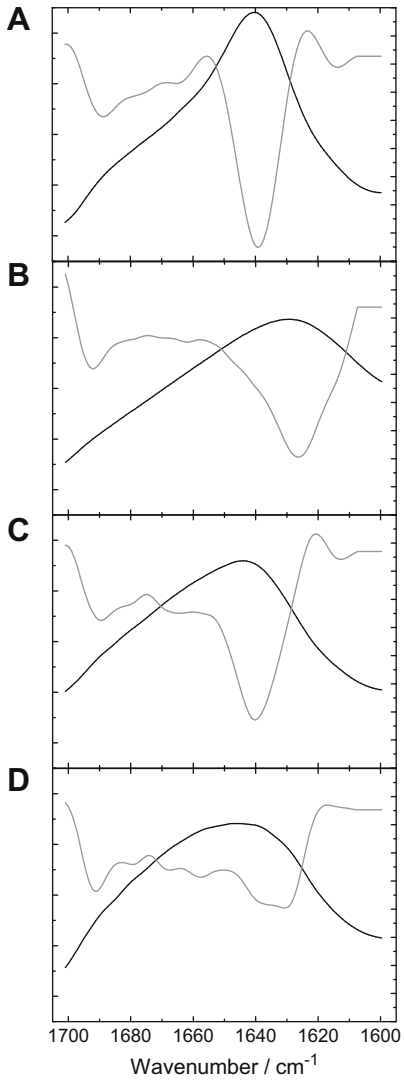

Fig. 1. ATR–FTIR adsorption spectra (black) and second derivates (light gray) of IgG1 (A), IgG1 after thermal stress (95 °C, 1 h) (B), immobilized IgG1 (C), and immobilized IgG1 after thermal stress (95 °C, 1 h) (D).

This could be confirmed by comparing these spectra with thermally stressed sample spectra (95 °C for 1 h). Both stressed IgG1 in solution (Fig. 1B) and stressed immobilized IgG1 (Fig. 1D) samples showed clearly changes in their secondary structure, namely a substantial shift in wavelength for the main band compared to the initial, native samples. In the spectra of thermally treated protein, the band detected around 1620–1630 cm^{-1} originates from intermolecular antiparallel β-sheet formation [63], which are often observed during protein denaturation and aggregation. However, comparing coupled protein with uncoupled, i.e. free protein, one observes that the protein secondary structure is mainly unchanged (Fig. 1), thus leading to the conclusion that the protein structure mainly keeps its initial structural integrity.

3.2. Temperature influence on B_{22} of IgG1

The influence of temperature on B_{22} of IgG1 was tested in the range of 5–35 °C for two sodium chloride concentrations (10 and 150 mM) at pH 6.2 (Fig. 2). The investigated temperatures were kept well below the denaturation temperature of the IgG1 to consider only B_{22} of native IgG1 [64]. As seen in Fig. 2, protein–protein interactions, as assessed by B_{22}, were not significantly modified by

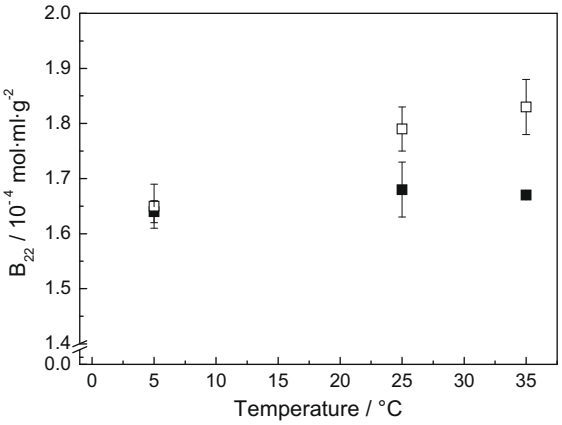

Fig. 2. Effect of temperature from 5 to 35 °C on B_{22} value of IgG1 in the presence of 5 mM sodium succinate pH 6.2: 10 mM NaCl (■) and 150 mM NaCl (□).

temperature at low salt concentration, whereas a temperature dependency was observed with increasing salt concentration up to 150 mM. Increasing the temperature slightly increased the repulsive interaction between the protein molecules. A similar trend has been described for lysozyme [54,65], which corresponds to lysozyme solubility enhancement by increasing temperature [66]. This is the case for temperatures well below the denaturation temperature of the protein. The experienced strong temperature dependency, reported by Piazza [67], is believed not to derive from electrostatic repulsions but more from hydrophobic interactions. The last interactions are known to depend strongly on temperature and mediate very short-ranged interparticle interactions [67]. The effect was enhanced in the presence of salt, which shields electrostatic interactions.

3.3. Effect of IgG1 protonation degree on B_{22}

Depending on the solution pH, protein molecules bear a net charge resulting from the sum of all charged ionized groups of the amino acids and carbohydrate structures of the protein. As the pH value approaches the protein's isoelectric point, the protein net charge diminishes. The protein net charge determines the electrostatic repulsions within its structure but also between different protein molecules in solution. On the one hand, a protein that is highly charged is affected by strong non-specific repulsions within its structure, which can destabilize its folded conformation [68]. On the other hand, charges on protein molecules enhance the intermolecular electrostatic repulsions and thus stabilize protein solution from a colloidal point of view [3]. In addition, protein solubility is known to be pH dependent, as it varies with the square of the protein net charge [69].

Based on the protein sequence, the protein net charge can be calculated as a function of the environmental pH with the EMBOSS software. The pH influence on B_{22} was measured using a mixed buffer system containing sodium acetate, sodium phosphate and sodium succinate to maintain a consistent buffer composition over the pH range of pH 4–8 (Fig. 3A). Increasing the pH value from 4 to 8 close to the IgG1 isoelectric point (ca. 8.3), the IgG1 net charges diminish and so B_{22}. As the protein net charge decreased, the repulsive interactions between protein molecules bearing the same charge are weakened. Thus, under alkaline pH conditions, the formation of attractive protein–protein interactions are more likely when compared to the repulsive interactions encountered under acidic pH conditions. The B_{22} value changed by only 0.6×10^{-4} mol ml g^{-2} between pH 4 and 8, which is rather small compared to the values obtained for similar conditions

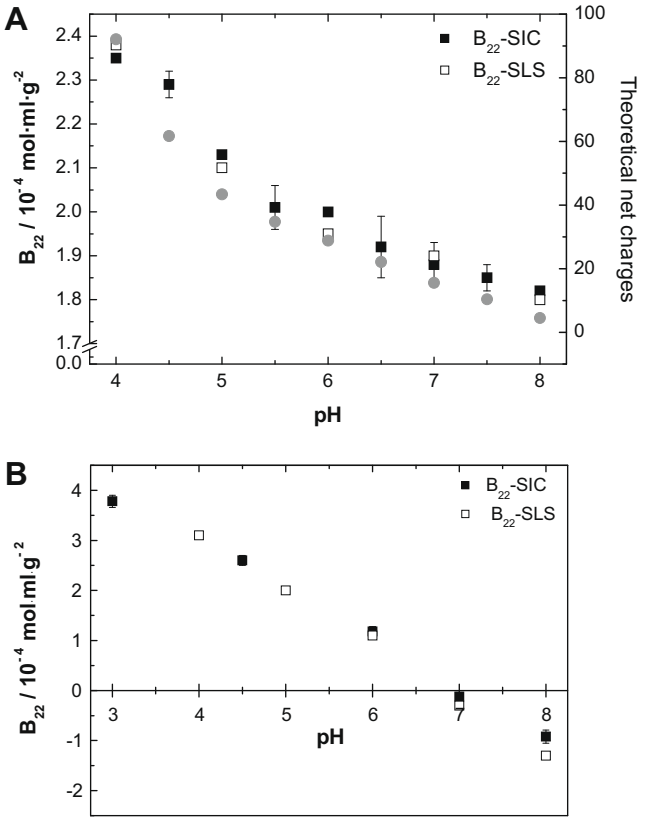

Fig. 3. (A) Influence of pH on IgG1 theoretical net charges calculated with the EMBOSS software (●) and B_{22} measured by SIC (■) and B_{22} measured by SLS (□) of a therapeutic IgG1 (10 mM sodium acetate, 10 mM sodium phosphate, 10 mM sodium succinate). (B) Influence of pH on lysozyme B_{22} measured by SIC (■) and B_{22} measured by SLS (□) (300 mM NaCl and 5 mM acetic acid at pH ⩽ 5 and 5 mM sodium phosphate at pH ⩾ 6).

for lysozyme [37] where a change of approximately $\Delta B_{22} = 4.5 \times 10^{-4}$ mol ml g^{-2} was detected (Fig. 3B). Additionally, the ionic strength of the buffer system limits the pH dependent change in B_{22}. In fact, the buffer ionic strength increased progressively by increasing pH, and the ionic strength was 3 times higher at pH 8 than at pH 4. Electrolytes modulate the strength of electrostatic interactions between the charged groups both within the protein and between protein molecules [3]. At low concentrations, salt ions shield protein charges, which reduce protein electrostatic repulsions. Indeed, according to Saluja et al., the influence of the pH on B_{22} of an IgG2 was considerably reduced by increasing the buffer ionic strength from 4 to 40 mM [11]. Increasing the buffer ionic strength could screen the repulsive interactions between protein charges and leveled B_{22} values. Consequently, at a constant weak ionic strength, B_{22} of IgG1 would decrease in a more pronounced manner by increasing pH. Increasing the pH value to IgG1's isoelectric point decreased intermolecular repulsive forces, even though the pH effect was modulated by the presence of buffer electrolytes, which screened protein charges.

3.4. Comparison of SIC and SLS-B_{22} data

B_{22} of IgG1 was also determined by SLS (Fig. 3A). B_{22} data derived from SIC and SLS were very similar. Both showed a slight regular decrease of B_{22} by increasing pH. The model was confirmed with lysozyme as second model protein (Fig. 3B).

A slight deviation was observed between lysozyme SIC and SLS data at negative B_{22} values, with the SLS-B_{22} data being slightly more negative. However, the pH trend for lysozyme remained very similar for both data sets (SIC-B_{22} and SLS-B_{22}). This was in accordance with Tessier et al. [37]. In contrast to the low pH influence of B_{22} for the tested IgG1, the pH impact on B_{22} for lysozyme is much more pronounced. For lysozyme, a change in B_{22} sign from positive to negative is induced at a pH of ca. 6.9 (Fig. 3B). Thus, below a pH of 6.9, attractive interactions between lysozyme molecules become dominant [59].

3.5. Influence of buffer composition on B_{22} of IgG1

The influence of the buffer species was studied with four different buffers (histidine, citrate, phosphate and succinate) in pharmaceutical relevant concentration ranges of 5–50 mM at a fixed pH of 6.2 (Fig. 4).

The presence of buffer can be essential in order to stabilize protein formulations, since buffer inhibits a change of pH in solution, which is a crucial factor for protein stability [70]. Furthermore, buffer ions may directly interact or even weakly bind to the protein. As shown in Fig. 4, B_{22} was sensitive to the buffer species, especially at low buffer concentrations. At 5 mM concentration, histidine showed the highest, positive B_{22} value (2.3×10^{-4} mol ml g^{-2}), whereas citrate and phosphate buffer had the lowest value (1.6×10^{-4} and 1.6×10^{-4} mol ml g^{-2} respectively). Increasing the buffer concentration diminished the difference between the buffer species until a similar B_{22} value of approx. 1.9×10^{-4} mol ml g^{-2} was reached for all tested buffers at 50 mM concentration. With increasing the histidine concentration B_{22} decreased, while increasing the other buffer concentration resulted in a slight increase of B_{22} or had no relevant influence. The three anionic buffers have a higher ionic strength compared to the histidine buffer at equivalent molar concentration and this may be one reason for the detected differences in B_{22}. Another aspect to consider is the binding of the excipient to the protein molecule. Katayama et al. observed slight differences in B_{22} values of IFN-tau in the presence of histidine, Tris or phosphate buffers at 20 mM [41] with $\Delta B_{22} \approx 0.2 \times 10^{-4}$ mol ml g^{-2}. These authors determined a very weak binding constant between histidine and IFN-tau of $K_b \approx 1 \times 10^2$ to 4×10^2 M^{-1} and discussed that probably this very weak binding may stabilize IFN-tau against thermally induced aggregation by increasing the difference between the changes of the free Gibbs energy of native and unfolded state (ΔG_{n-unf}). However, the mechanical reason for the stabilization effect is not discussed by Katayama et al. One aspect to consider is that the weak excipient binding has an impact on electrostatics in order to induce the observed effect.

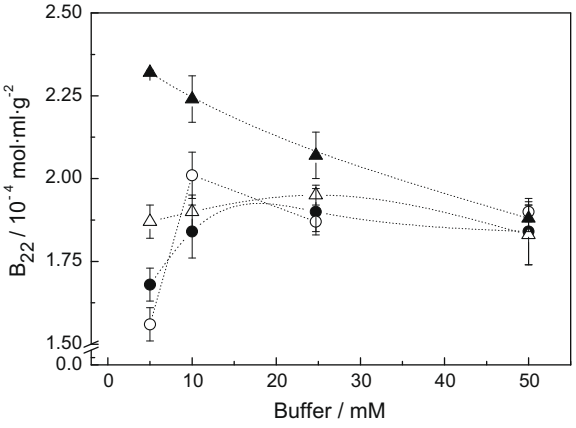

Fig. 4. Effect of buffer species at pH 6.2 on B_{22} value of IgG1: histidine (▲), succinate (△), citrate (●) and phosphate (○) as a function of buffer concentration.

The basically buffer independent impact on B_{22} indicates that a colloidal stabilization mechanism is of minor importance to understand the IFN-tau stabilization effect in the presence of histidine. Based on the obtained B_{22} data, the buffer species had a stronger impact on antibody–antibody interactions compared to the interactions observed for IFN-tau. Overall, the buffer concentration should be chosen such that it is high enough to control and stabilize the formulation pH, but as low as possible to create solution conditions with repulsive protein–protein interactions (i.e. strong positive B_{22} values are expected).

3.6. Influence of sodium chloride on B_{22} of IgG1

The influence of sodium chloride was tested in the concentration range of 0–150 mM in the presence of 5 mM sodium succinate at pH 6.2, since NaCl is commonly added to obtain isotonic drug solutions and to adjust the ionic strength. Up to a concentration of 100 mM, NaCl had little influence on B_{22} (Fig. 5) for the investigated antibody. Further, increasing the NaCl concentration to 150 mM decreases B_{22} reflecting the fact that ionic screening reduces the repulsive charge effect and/or repulsive charge interactions between protein molecules. Thus, protein–protein colloidal stability is favored under low ionic strength.

Indeed, electrostatic repulsive forces usually decrease with addition of salt ions due to their inverse dependence on ionic strength [71]. It corresponds to a similar effect reported for two humanized monoclonal antibodies of the same subtype (IgG1) [40]. In both cases, the decrease in B_{22} value was not strong enough to reach negative B_{22} values, revealing less favorable repulsive particle conditions in the presence of higher salt concentration. Consequently, for the presented case study, the addition of up to 50–100 mM NaCl barely perturbed the IgG1 intermolecular interactions. As a consequence, sodium chloride can be used as isotonic agent without increasing the propensity of the formation of protein associates.

3.7. Influence of amino acids on B_{22} of IgG1

Amino acids are commonly used as solvent additive in protein purification and as excipients for protein formulations. Arginine, glycine and histidine are the amino acids most frequently utilized to stabilize protein formulations, in some cases to improve protein solubility and to avoid protein aggregation [72]. The influence of arginine, glycine, histidine and methionine was tested in the concentration range of 0–100 mM in the presence of 5 mM sodium succinate at in pH 6.2. The addition of glycine or methionine did not influence B_{22}, whereas histidine and arginine induced changes (Fig. 6). Both, arginine and histidine, acted differently on B_{22} depending on their concentrations in solution compared to methionine and glycine. The presence of arginine and histidine at 5–10 mM induces a decrease in B_{22}, which is more pronounced for arginine. However, buffer concentrations equal or higher than 20 mM led to a slight B_{22} increase. Most amino acids are described to stabilize proteins by the mechanism of preferential exclusion of the excipient from the protein surface [72]. Stabilization via preferential exclusion was reflected by constant B_{22} values by titrating methionine or glycine to the protein, where no excipient-protein binding is observed. Histidine and arginine presented a different B_{22} profile and both amino acids are reported to weakly bind to proteins [41,73].

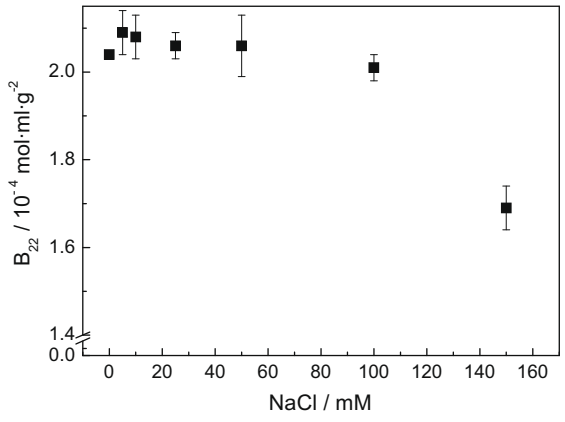

Fig. 5. Effect of NaCl on B_{22} value of IgG1 in the presence of 5 mM sodium succinate pH 6.2.

The influence of the amino acid side chain structure has been studied by Shiraki et al. with lysozyme as model protein [74] at pH 6.5 in 50 mM sodium phosphate buffer in order to avoid protein aggregation. Positively charged amino acids were more effective than hydrophobic and negatively charged amino acids to prevent heat-induced and dilution-induced protein aggregation. Arginine presented the most pronounced effect. Increasing the arginine concentration enhanced its preventive action [74] and a maximal effect was obtained at 300 mM. Furthermore, the most substantial preventive effect of arginine against aggregation was confirmed with various proteins of different pI and molecular weights [74]. According to Arakawa et al., the protective effect of arginine against heat-induced aggregation results from its interaction with the peptide back bonds and most amino acid side chains (both hydrophobic and hydrophilic), especially tyrosine and tryptophan [73] leading to a reduction of both electrostatic (hydrogen bonding and ionic interactions) and hydrophobic interactions. One has to mention that the used arginine concentration is often very high in the range of 0.2–1 M. Histidine also presented the property to bind to protein, but its binding was reported to be very weak ($K_b \approx 1 \times 10^2$ to $4 \times 10^2\ M^{-1}$) [41]. Its effect on thermodynamic stabilization of IFN-tau [41] and EPO [75] was preponderant. Thus, at low amino acid concentrations (up to 10 mM) the B_{22} decrease might reflect arginine or histidine binding or changes of the hydration property of the IgG1 molecules. The B_{22} decrease was stronger in the presence of arginine when compared to histidine, which could reflect the stronger binding of arginine to protein surface. At higher concentration, all amino acids act similarly, corresponding to the protective and solubilization effect due to preferential exclusion.

3.8. Stability of 20 mg/ml IgG1 solutions at 40 °C

A stability study of 20 mg/ml IgG solutions was conducted for 12 weeks at 40 °C as a function of buffer species and concentration at pH 6.2 comparing sodium citrate, histidine, sodium phosphate and sodium succinate at both 5 and 50 mM. Turbidity was measured as well as the formation of soluble aggregates (by SE-HPLC). It is obvious that the turbidity increased was more pronounced for the histidine buffer formulations (5 and 50 mM) (Fig. 7A and 7B) compared to the other three buffer formulations. The 5 mM histidine formulation presented a significant turbidity increase after 12 weeks, whereas the turbidity of the 50 mM histidine formulation had already increased significantly after 4 weeks. The increase in turbidity is accompanied by a yellow discoloration of the histidine formulation. This solution discoloration is also apparent for the histidine buffer solutions (in the absence of protein) stored under the same conditions. This led to the conclusion of chemical instabilities of the histidine buffer. Histidine is susceptible to oxidation either by photocatalyzed or by metal-ion-catalyzed mechanisms [76,77]. It is mainly oxidized to 2-oxo-histidine, aspartic acid and asparagines [76,77]. Therefore to avoid the chemical instability

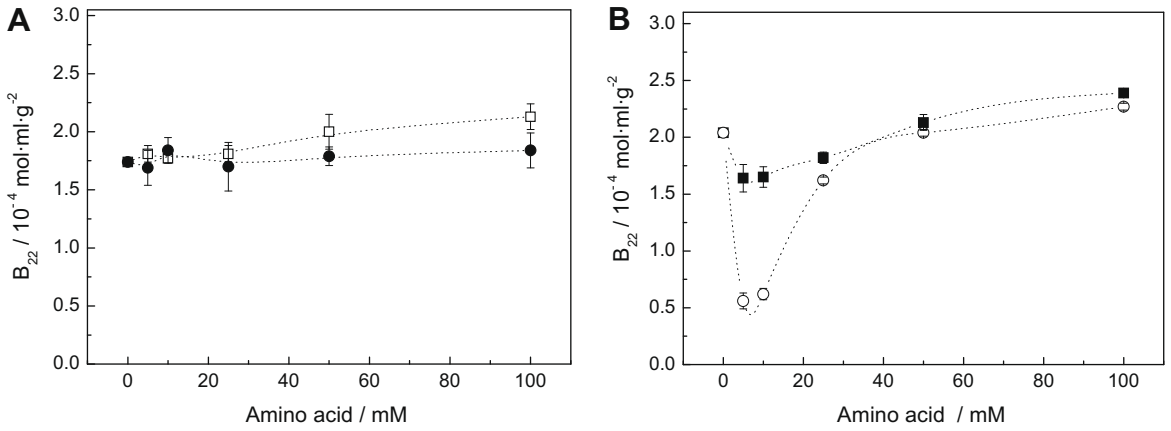

Fig. 6. Effect of amino acids on B_{22} of IgG1 in the presence of 5 mM sodium succinate pH 6.2: (A) methionine (●) and glycine (□), (B) arginine (○) and histidine (■).

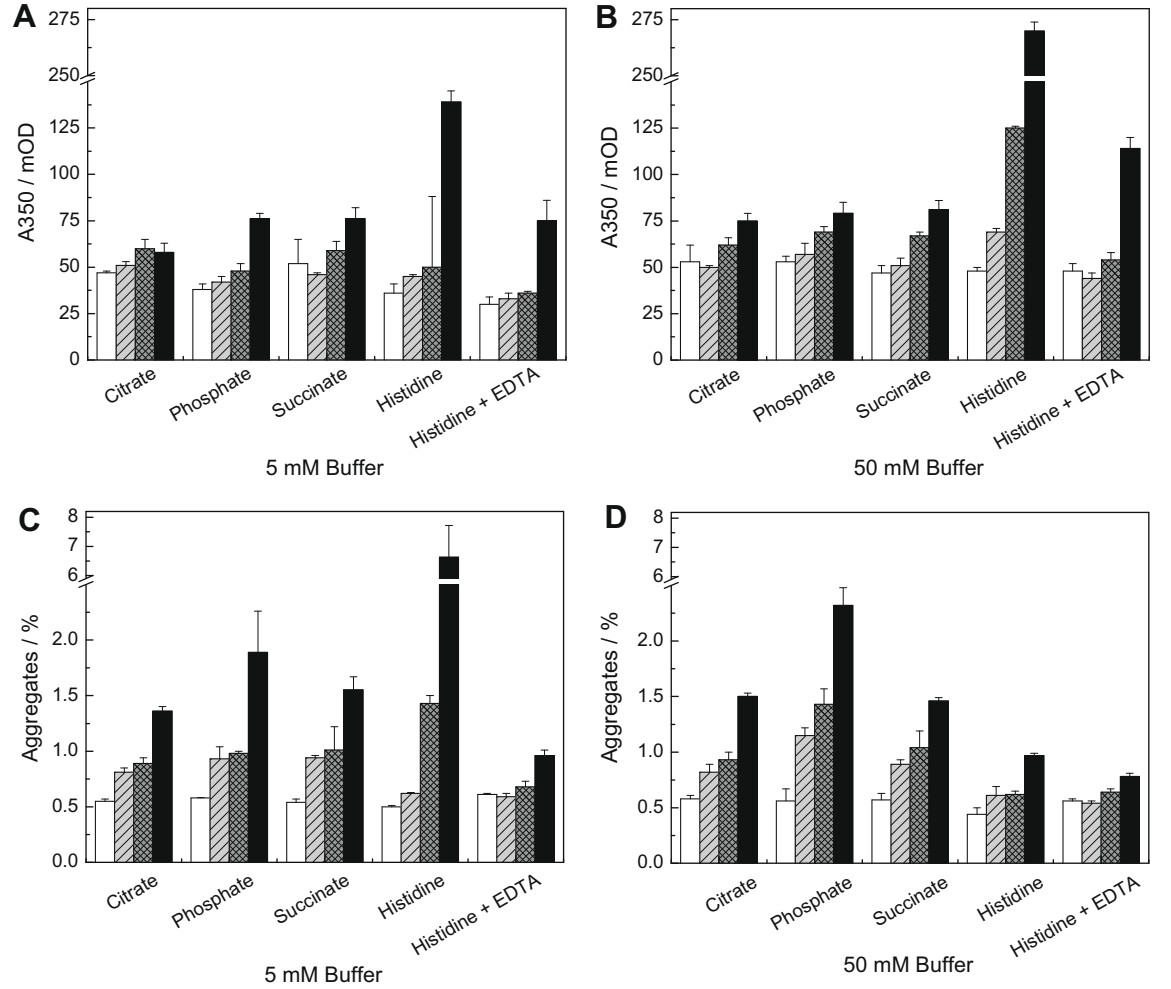

Fig. 7. Turbidity (A and B) and soluble aggregates as measured by SE-HPLC (C and D) of 5 mM and 50 mM buffer pH 6.2 containing IgG1 solutions (20 mg/ml) before (blank columns) and after 1 week (light gray columns), 4 weeks (gray columns) and 12 weeks (black columns) storage at 40 °C.

of the buffer, 20 μM EDTA (ethylenediaminetetraacetic acid) were added to the 20 mg/ml IgG1 histidine solution, even though no metal ions could be detected by atomic absorption spectroscopy (<0.02 mg/g) [78].

The addition of 20 μM EDTA to the histidine-containing samples inhibited the solution discoloration during the 12-week storage and the increase in turbidity was better controlled. The 5 mM histidine solution presented a similar increase in turbidity as the other tested buffers, whereas the turbidity increase remained higher for the 50 mM histidine/EDTA solution (Fig. 7).

The soluble aggregate content was kept below 2% for the majority of the tested formulations (Fig. 7C and D). The 5 mM histidine-containing formulation showed the highest amount in soluble aggregates (6.6%), but it could be stabilized by the presence of

EDTA. Indeed this latter solution presented the lowest increase in soluble aggregates (1%) after 12 weeks at 40 °C within the 5 mM buffers. The two 50 mM histidine-containing formulations did not present a substantially increased level of soluble aggregates after 12 weeks at 40 °C, but they presented higher turbidity compared to other buffer formulations indicating a higher propensity and equilibrium shift to the formation of insoluble aggregates. Matheus et al. [79] showed for higher histidine buffer concentrations (10 and 50 mM at pH 6.0) that the formation of medium to large size aggregates of cetuximab was favored under elevated thermal storage conditions that were responsible for higher solution turbidity. However, histidine did not influence the soluble aggregate content.

When its buffer chemical instability was controlled by the presence of the chelating excipient, the formulation containing 5 mM histidine was a well-stabilizing protein formulation buffer. Histidine has been already reported to stabilize IFN-tau better than phosphate or Tris buffer [41]. Its mechanism of stabilization was attributed to conformational stabilization by weak binding to the native protein state and to a lesser extent to colloidal stabilization.

The B_{22} coefficient of IgG1 was slightly increased in the presence of histidine at low concentration in comparison with the other buffer systems. This was also confirmed by the study of Katayama et al. [41]. However, the ability of histidine to increase the repulsive interactions in solution may not be the only mechanism leading to the best IgG1 stabilization. The conformational stability of the protein seemed to be improved as well. The DSC thermograms of the histidine-containing formulations (Fig. 8A) presented two peaks representing the Fab and the Fc fragment, the Fab fragment having the larger experimental enthalpy [64,80]. The DSC thermograms of IgG1 in the other buffers (exemplarily shown for 5 mM sodium phosphate buffer in Fig. 8B) presented only the first peak followed by a sudden decrease of the signal and a shift of the baseline corresponding to IgG1 aggregation and precipitation at its thermal unfolding. Correspondingly, in 5 mM histidine buffer the IgG1 exhibited the highest Tm (expressed as the maximum of the heat capacity curve), whereas the Tm values for the other buffers were in a comparable range (Fig. 8C). The negligible impact of buffer composition at pH 6.2 on Tm was comparable to the results reported with cetuximab [79] and a recombinant human megakaryocyte growth factor [81]. High buffer concentration did not improve IgG1 stability. This could reflect the self-buffering action of monoclonal antibodies in the pH range of 4–6 provided by the proteins' charged amino acids including aspartic acid, glutamic acid and histidine [82].

Thus, 5 mM histidine buffer in which the IgG1 showed the highest B_{22} value was in combination with EDTA the most promising candidate for formulating the investigated IgG1.

3.9. Colloidal stability of 20 mg/ml IgG1 solutions

The colloidal stability of 20 mg/ml IgG1 formulations was tested as a function of the buffer species (5 mM, pH 6.2) by measuring solution turbidity after stirring stress. The histidine formulation having the highest positive B_{22} value (2.3×10^{-4} mol ml g^{-2}) corresponded to the slowest turbidity increase (Fig. 9). Both formulations having the same, but lower B_{22} value (1.6×10^{-4} mol ml g^{-2}), namely sodium citrate and sodium phosphate formulations, showed a similar trend accompanied by a larger colloidal instability compared to the histidine formulation. This result confirmed the ability of histidine to better stabilize IgG1.

Protein solutions presenting lower B_{22} values, or even negative B_{22} values [59] showed a lower colloidal stability. Therefore, higher (positive) B_{22} values should be favored to reach higher protein stability, especially for cases where protein stability/instability is governed by protein colloidal stability.

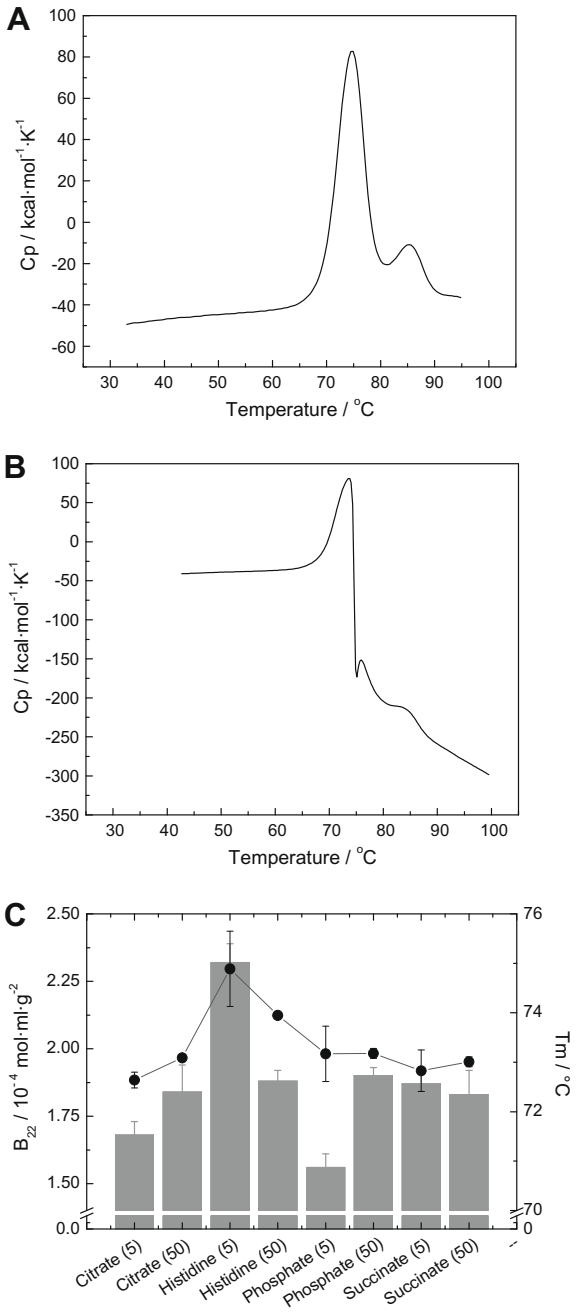

Fig. 8. DSC thermograms of IgG1 in 5 mM histidine buffer (A) and in 5 mM sodium phosphate buffer (B) at pH 6.2 and comparison of B_{22} (gray column) value to Tm value (black solid circle) (C).

4. Conclusions

Fourier transform infrared spectroscopy spectra did not reveal any relevant structural changes of immobilized IgG1 compared to the initial antibody solution. Based on this statement, self-interaction chromatography measures the interactions between native IgG1 in solution and native like immobilized IgG1, and thus allowed B_{22} determination.

Small variations in B_{22} values were measurable by varying physiologically relevant formulation parameters. Under all the tested conditions, B_{22} remained positive for the investigated antibody, indicating all tested formulations favored repulsive interactions. Formulation parameters having the most impact on B_{22}

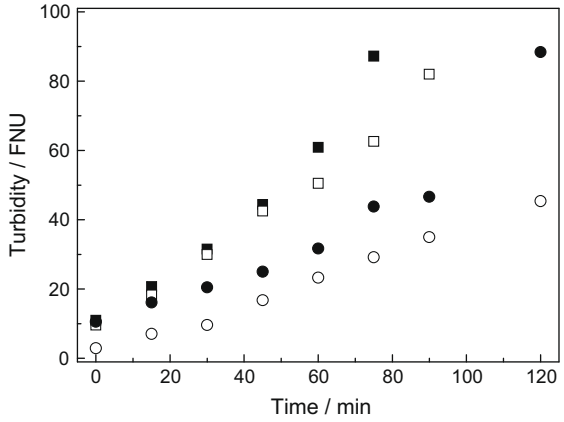

Fig. 9. Turbidity of 20 mg/mL IgG1 solutions during stirring at 1200 rpm at 25 °C as a function of time at different buffers pH 6.2: 5 mM Na-citrate (■) (B_{22} 1.6×10^{-4} mol ml g^{-2}), 5 mM Na-phosphate (□) (B_{22} 1.6×10^{-4} mol ml g^{-2}), 5 mM Na-succinate (●) (B_{22} 1.9×10^{-4} mol ml g^{-2}) and 5 mM histidine (○) (B_{22} 2.3×10^{-4} mol ml g^{-2}).

were pH and ionic strength for the investigated antibody (isoelectric point of ca. 8.3). Buffer species influenced only at low ionic strength (<10 mM), whereas salt and amino acid played a role at high concentration.

According to B_{22}, the 5 mM histidine-containing buffer formulation showed a higher potential to favor repulsive protein–protein interactions. Probably, the presence of histidine has an impact on electrostatic and/or hydration properties of the protein, which lead to repulsive interactions. This corresponded to slightly superior IgG1 stability upon 12-week storage at 40 °C at 20 mg/ml, when the chemical instability of histidine was eliminated by EDTA addition. However, the colloidal stabilization did not seem to be the only factor influencing the protein stability, and the conformational stability has also to be considered.

Self-interaction chromatography gave reliable results of IgG1–IgG1 interactions, when compared to results derived from static light scattering, depending on solution parameters predicting formulation parameters to increase IgG1 colloidal stability. Thus, self-interaction chromatography appears to be a relevant high throughput screening method, combined with lab-automation, for the physical characterization of therapeutic proteins and the optimization of their formulation.

Such approaches allow the implementation of a more rational formulation design in pharmaceutical biotechnology. However, it is important to confirm these results by using other immunoglobulins.

Acknowledgments

The authors would like to thank H. Schott, I. Miller and T. Hennes for excellent technical assistance and Boehringer Ingelheim Pharma GmbH & Co. KG for financial support.

References

[1] S.J. Shire, Z. Shahrokh, J. Liu, Challenges in the development of high protein concentration formulations, J. Pharm. Sci. 93 (6) (2004) 1390–1402.
[2] W. Wang, S. Singh, D.L. Zeng, K. King, S. Nema, Antibody structure, instability, and formulation, J. Pharm. Sci. 96 (1) (2007) 1–26.
[3] E.Y. Chi, S. Krishnan, T.W. Randolph, J.F. Carpenter, Physical stability of proteins in aqueous solution: mechanism and driving forces in nonnative protein aggregation, Pharm. Res. 20 (9) (2003) 1325–1336.
[4] B.M. Baynes, B.L. Trout, Rational design of solution additives for the prevention of protein aggregation, Biophys. J. 87 (2004) 1631–1639.
[5] R.A. Broglia, G. Tiana, S. Pasquali, H.E. Roman, E. Vigezzi, Folding and aggregation of designed proteins, Proc. Natl. Acad. Sci. USA 95 (1998) 12930–12933.
[6] K. Dudgeon, K. Famm, D. Christ, Sequence determinants of protein aggregation in human VH domains, Protein Eng. 22 (3) (2009) 217–220.
[7] A. Trovato, F. Senol, S.C.E. Tosatto, The PASTA server for protein aggregation prediction, Protein Eng. 20 (10) (2007) 521–523.
[8] N. Harn, C. Allan, C. Oliver, C.R. Middaugh, Highly concentrated monoclonal antibody solutions: direct analysis of physical structure and thermal stability, J. Pharm. Sci. 96 (3) (2007) 532–546.
[9] P. Garidel, H. Schott, Fourier-transform midinfrared spectroscopy for analysis and screening of liquid protein formulations. Part 2: detailed analysis and applications, BioProcess Int. 4 (2006) 48–55.
[10] J.R. Alford, S.C. Kwok, J.N. Roberts, D.S. Wuttke, B.S. Kendrick, J.F. Carpenter, T.W. Randolph, High concentration formulations of recombinant human interleukin-1 receptor antagonist: I. Physical characterization, J. Pharm. Sci. 97 (8) (2008) 3035–3050.
[11] A. Saluja, A.V. Badkar, D.L. Zeng, S. Nema, D.S. Kalonia, Ultrasonic storage modulus as a novel parameter for analyzing protein–protein interactions in high protein concentration solutions: correlation with static and dynamic light scattering measurements, Biophys. J. 92 (1) (2007) 234–244.
[12] M. Jimenez, G. Rivas, A.P. Minton, Quantitative characterization of weak self-association in concentrated solutions of immunoglobulin G via the measurement of sedimentation equilibrium and osmotic pressure, Biochemistry 46 (28) (2007) 8373–8378.
[13] C.A. Haynes, K. Tamura, H.R. Korfer, H.W. Blanch, J.M. Prausnitz, Thermodynamic properties of aqueous alpha-chymotrypsin solutions from membrane osmometry measurements, J. Phys. Chem. 96 (2) (1992) 905–912.
[14] H. Bajaj, V.K. Sharma, D.S. Kalonia, Determination of second virial coefficient of proteins using a dual-detector cell for simultaneous measurement of scattered light intensity and concentration in SEC-HPLC, Biophys. J. 87 (2004) 4048–4055.
[15] M. Deszczynski, S.E. Harding, D.J. Winzor, Negative second virial coefficients as predictors of protein crystal growth: evidence from sedimentation equilibrium studies that refutes the designation of those light scattering parameters as osmotic virial coefficients, Biophys. Chem. 120 (2006) 106–113.
[16] P.M. Tessier, S.I. Sandler, A.M. Lenhoff, Direct measurement of protein osmotic second virial cross coefficients by cross-interaction chromatography, Protein Sci. 13 (2004) 1379–1390.
[17] D.J. Winzor, M. Deszczynski, S.E. Harding, P.R. Wills, Nonequivalence of second virial coefficients from sedimentation equilibrium and static light scattering studies of protein solutions, Biophys. Chem. 128 (2007) 46–55.
[18] D.J. Winzor, D.J. Scott, P.R. Wills, A simpler analysis for the measurement of second virial coefficients by self-interaction chromatography, Anal. Biochem. 371 (2007) 21–25.
[19] J. Lebowitz, M.S. Lewis, P. Schuck, Modern analytical ultracentrifugation in protein science: A tutorial review, Protein Sci. 11 (2002) 2067–2079.
[20] A.P. Minton, Alternative strategies for the characterization of associations in multicomponent solutions via measurement of sedimentation equilibrium, Prog. Colloid Polym. Sci. 107 (1997) 11–19.
[21] A.P. Minton, Quantitative characterization of reversible macromolecular associations via sedimentation equilibrium: an introduction, Exp. Mol. Med. 32 (2000) 1–5.
[22] S. Beeckmans, Chromatographic methods to study protein–protein interactions, Methods 19 (1999) 278–305.
[23] J. Bloustine, V. Berejnov, S. Fraden, Measurements of protein–protein interactions by size-exclusion chromatography, Biophys. J. 85 (2003) 1619–1632.
[24] R. Hahn, K. Amatschek, E. Schallaun, R. Necina, Performance of affinity chromatography with peptide ligands: influence of spacer, matrix composition and immobilization chemistry, Int. J. Bio-Chromatogr. 5 (3) (2000) 175–185.
[25] E. Heftmann, Chromatography: Fundamentals and Applications of Chromatography and Related Differential Migration Methods: Applications, Elsevier, 2004.
[26] R. Lemque, A. Jaulmes, B. Sebile, C. Vidal-Madjar, Study of the adsorption of self-associating proteins on an anion exchanger: application to the chromatography of β-lactoglobulin B, J. Chromatogr. 599 (1992) 255–265.
[27] F.J. Stevens, Analysis of protein–protein interaction by simulation of small-zone size-exclusion chromatography: application to an antibody–antigen association, Biochemistry 25 (5) (1986) 981–993.
[28] J. Wen, T. Arakawa, J.S. Philo, Size-exclusion chromatography with on-line light scattering, absorbance, and refractive index detectors for studying proteins and their interactions, Anal. Biochem. 240 (1996) 155–166.
[29] D.J. Winzor, The development of chromatography for the characterization of protein interactions: a personal perspective, Biochem. Soc. Trans. 31 (5) (2003) 1010–1014.
[30] S.Y. Patro, T.M. Przybycien, Self-interaction chromatography: a tool for the study of protein–protein interactions in bioprocessing environments, Biotechnol. Bioeng. 52 (1996) 193–203.
[31] T.M. Przybycien, Protein–protein interactions as a means of purification, Curr. Opin. Biotechnol. 9 (1998) 164–170.
[32] P.M. Tessier, S.D. Vandrey, B.W. Berger, R. Pazhianur, S.I. Sandler, A.M. Lenhoff, Self-interaction chromatography: a novel screening method for rational protein crystallization, Acta Crystallogr. D: Biol. Crystallogr. 58 (2002) 1531–1535.
[33] F. Bonnete, S. Finet, A. Tardieu, Second virial coefficient: variations with lysozyme crystallization conditions, J. Cryst. Growth 196 (2–4) (1999) 403–414.

[34] W. Liu, D. Bratko, J.M. Prausnitz, H.W. Blanch, Effect of alcohols on aqueous lysozyme–lysozyme interactions from static light-scattering measurements, Biophys. Chem. 107 (3) (2004) 289–298.
[35] B.L. Neal, D. Asthagiri, O.D. Velev, A.M. Lenhoff, Why is the osmotic second virial coefficient related to protein crystallization?, J Cryst. Growth 196 (1999) 377–387.
[36] D.H. Johnson, A. Parupudi, W.W. Wilson, L.J. Delucas, High-throughput self-interaction chromatography: applications in protein formulation prediction, Pharm. Res. 26 (2) (2009) 269–305.
[37] P.M. Tessier, A.M. Lenhoff, S.I. Sandler, Rapid measurement of protein osmotic second virial coefficients by self-interaction chromatography, Biophys. J. 82 (3) (2002) 1620–1631.
[38] P.M. Tessier, H.R. Johnson, R. Pazhianur, B.W. Berger, Predictive crystallization of ribonuclease A via rapid screening of osmotic second virial coefficients, Proteins 50 (2003) 303–311.
[39] T. Ahamed, B.N.A. Esteban, M. Ottens, G.W.K. van Dedem, L.A.M. van der Wielen, M.A.T. Bisschops, A. Lee, C. Pham, J. Thommes, Phase behavior of an intact monoclonal antibody, Biophys. J. 93 (2) (2007) 610–619.
[40] J. Liu, M.D. Nguyen, J.D. Andya, S.J. Shire, Reversible self-association increases the viscosity of a concentrated monoclonal antibody in aqueous solution, J. Pharm. Sci. 94 (9) (2005) 1928–1940.
[41] D.S. Katayama, R. Nayar, D.K. Chou, J.J. Valente, J. Cooper, C.S. Henry, D.G. Vander Velde, L. Villarete, C.P. Liu, M.C. Manning, Effect of buffer species on the thermally induced aggregation of interferon-tau, J. Pharm. Sci. 95 (6) (2006) 1212–1226.
[42] H. Bajaj, V.K. Sharma, A. Badkar, D. Zeng, S. Nema, D.S. Kalonia, Protein structural conformation and not second virial coefficient relates to long-term irreversible aggregation of a monoclonal antibody and ovalbumin in solution, Pharm. Res. 23 (6) (2006) 1382–1394.
[43] E.Y. Chi, S. Krishnan, B.S. Kendrick, B.S. Chang, J.F. Carpenter, T.W. Randolph, Roles of conformational stability and colloidal stability in the aggregation of recombinant human granulocyte colony-stimulating factor, Protein Sci. 12 (5) (2003) 903–913.
[44] J.R. Alford, B.S. Kendrick, J.F. Carpenter, T.W. Randolph, Measurement of the second osmotic virial coefficient for protein solutions exhibiting monomer–dimer equilibrium, Anal. Biochem. 377 (2) (2008) 128–133.
[45] C. Haas, J. Drenth, W.W. Wilson, Relation between the solubility of proteins in aqueous solutions and the second virial coefficient of the solution, J. Phys. Chem. B 103 (14) (1999) 2808–2811.
[46] V. Le Brun, W. Friess, T. Schultz-Fademrecht, S. Muehlau, P. Garidel, Lysozyme–lysozyme self-interactions as assessed by the osmotic second virial coefficient: impact for physical protein stabilisation, Biotechnol. J. 4 (9) (2009) 1305–1319.
[47] E.R.A. Lima, E.C. Biscaia, M. Bostrom, F.W. Tavares, Osmotic second virial coefficients and phase diagrams for aqueous proteins from a much-improved Poisson–Boltzmann equation, J. Phys. Chem. C 111 (2007) 16055–16059.
[48] R.W. Payne, R. Nayar, R. Tarantino, S. Del Terzo, J. Moschera, J. Di, D. Heilman, B. Bray, M.C. Manning, C.S. Henry, Second virial coefficient determination of a therapeutic peptide by self-interaction chromatography, Biopolymers 84 (5) (2006) 527–533.
[49] S. Ruppert, S.I. Sandler, A.M. Lenhoff, Correlation between the osmotic second virial coefficient and the solubility of proteins, Biotechnol. Prog. 17 (1) (2001) 182–187.
[50] D. Stigter, T.L. Hill, Theory of the Donnan membrane equilibrium 2. Calculation of the osmotic pressure and of the salt distribution in a Donnan system with highly charged colloid particles, J. Phys. Chem. 63 (1959) 551–556.
[51] J. Wanka, W. Peukert, Die Bedeutung des zweiten osmotischen Virialkoeffizienten für die Proteinkristallization, Chem. Ing. Tech. 2996 (2008) 273–278.
[52] P. Garidel, H. Schott, Fourier-transform midinfrared spectroscopy for analysis and screening of liquid protein formulations. Part 1: understanding infrared spectroscopy of proteins, BioProcess Int. 4 (5) (2006) 40–46.
[53] P.M. Tessier, A.M. Lenhoff, Measurements of protein self-association as a guide to crystallization, Curr. Opin. Biotechnol. 14 (2003) 512–516.
[54] J.J. Valente, R.W. Payne, M.C. Manning, W.W. Wilson, C.S. Henry, Colloidal behavior of proteins: effects of the second virial coefficient on solubility, crystallization and aggregation of proteins in aqueous solution, Curr. Pharm. Biotechnol. 6 (6) (2005) 427–436.
[55] J.J. Valente, K.S. Verma, M.C. Manning, W.W. Wilson, C.S. Henry, Second virial coefficient studies of cosolvent-induced protein self-interaction, Biophys. J. 89 (2005) 4211–4218.
[56] O.D. Velev, E.W. Kaler, A.M. Lenhoff, Protein interactions in solution characterized by light and neutron scattering: comparison of lysozyme and chymotrypsinogen, Biophys. J. 75 (1998) 2682–2697.
[57] P. Rice, I. Longden, A. Bleasby, EMBOSS: the European molecular biology open software suite, Trends Genet. 16 (6) (2000) 276–277.
[58] H.C. Mahler, R. Muller, W. Friess, A. Delille, S. Matheus, Induction and analysis of aggregates in a liquid IgG1-antibody formulation, Eur. J. Pharm. Biopharm. 59 (3) (2005) 407–417.
[59] V. Le Brun, W. Friess, S. Bassarab, P. Garidel, Correlation of protein–protein interactions as assessed by affinity chromatography with colloidal stability: a case study with lysozyme, Pharm. Dev. Technol. (2010), doi:10.1080/10837450903262074.
[60] J. Bandekar, Amide modes and protein conformation, Biochim. Biophys. Acta 1120 (2) (1992) 123–143.
[61] D.M. Byler, H. Susi, Examination of the secondary structure of proteins by deconvolved FTIR spectra, Biopolymers 25 (3) (1986) 469–487.
[62] A.C. Dong, B. Kendrick, L. Kreilgard, J. Matsuura, M.C. Manning, J.F. Carpenter, Spectroscopic study of secondary structure and thermal denaturation of recombinant human factor XIII in aqueous solution, Arch. Biochem. Biophys. 347 (2) (1997) 213–220.
[63] M. van de Weert, P.I. Haris, W.E. Hennink, D.J.A. Crommelin, Fourier transform infrared spectrometric analysis of protein conformation: effect of sampling method and stress factors, Anal. Biochem. 297 (2) (2001) 160–169.
[64] C. Hoffmann, A. Blume, I. Miller, P. Garidel, Insights into protein–polysorbate interactions analysed by means of isothermal titration and differential scanning calorimetry, Eur. Biophys. J. 38 (5) (2009) 557–568.
[65] C. Gripon, L. Legrand, I. Rosenman, O. Vidal, M.C. Robert, F. Boue, Lysozyme–lysozyme interactions in under- and super-saturated solutions: a simple relation between the second virial coefficients in H_2O and D_2O, J. Cryst. Growth 178 (4) (1997) 575–584.
[66] C. Gripon, L. Legrand, I. Rosenman, O. Vidal, M.C. Robert, F. Boue, Lysozyme solubility in H_2O and D_2O solutions: a simple relationship, J. Cryst. Growth 177 (1997) 238–247.
[67] R. Piazza, Protein interactions and association: an open challenge for colloid science, Curr. Opin. Colloid Interface Sci. 8 (6) (2004) 515–522.
[68] K.A. Dill, Dominant forces in protein folding, Biochemistry 29 (31) (1990) 7133–7155.
[69] K.L. Shaw, G.R. Grimsley, G.I. Yakovlev, A.A. Makarov, C.N. Pace, The effect of net charge on the solubility, activity, and stability of ribonuclease Sa, Protein Sci. 10 (6) (2001) 1206–1215.
[70] N. Wang, B. Hu, R. Ionescu, H. Mach, J. Sweeney, C. Hamm, M.J. Kirchmeier, B.K. Meyer, Opalescence of an IgG1 monoclonal antibody formulation is mediated by ionic strength and excipients, BioPharm. Int. 22 (2009) 36–47.
[71] A. Saluja, D.S. Kalonia, Nature and consequences of protein–protein interactions in high protein concentration solutions, Int. J. Pharm. 358 (1–2) (2008) 1–15.
[72] T. Arakawa, K. Tsumoto, Y. Kita, B. Chang, D. Ejima, Biotechnology applications of amino acids in protein purification and formulations, Amino Acids 33 (4) (2007) 587–605.
[73] T. Arakawa, D. Ejima, K. Tsumoto, N. Obeyama, Y. Tanaka, Y. Kita, S.N. Timasheff, Suppression of protein interactions by arginine: a proposed mechanism of the arginine effects, Biophys. Chem. 127 (1-2) (2007) 1–8.
[74] K. Shiraki, M. Kudou, S. Fujiwara, T. Imanaka, M. Takagi, Biophysical effect of amino acids on the prevention of protein aggregation, J. Biochem. 132 (4) (2002) 591–595.
[75] T. Arakawa, J.S. Philo, Y. Kita, Kinetic and thermodynamic analysis of thermal unfolding of recombinant erythropoietin, Biosci. Biotechnol. Biochem. 65 (6) (2001) 1321–1327.
[76] P.M. Bummer, Chemical considerations in protein and peptide stability, Drugs Pharm. Sci. 175 (2008) 7–42.
[77] J.L. Reubsaet, J.H. Beijnen, A. Bult, R.J. van Maanen, J.A. Marchal, W.J. Underberg, Analytical techniques used to study the degradation of proteins and peptides: chemical instability, J. Pharm. Biomed. Anal. 17 (6–7) (1998) 955–978.
[78] B. Chen, R. Bautista, K. Yu, G.A. Zapata, M.G. Mulkerrin, S.M. Chamow, Influence of histidine on the stability and physical properties of a fully human antibody in aqueous and solid forms, Pharm. Res. 20 (12) (2003) 1952–1960.
[79] S. Matheus, H.C. Mahler, W. Friess, A critical evaluation of Tm (FTIR) measurements of high-concentration IgG(1) antibody formulations as a formulation development tool, Pharm. Res. 23 (7) (2006) 1617–1627.
[80] R.M. Ionescu, J. Vlasak, C. Price, M. Kirchmeier, Contribution of variable domains to the stability of humanized IgG1 monoclonal antibodies, J. Pharm. Sci. 97 (4) (2008) 1414–1426.
[81] L.O. Narhi, J.S. Philo, B. Sun, B.S. Chang, T. Arakawa, Reversibility of heat-induced denaturation of the recombinant human megakaryocyte growth and development factor, Pharm. Res. 16 (6) (1999) 799–807.
[82] Y.R. Gokarn, E. Kras, C. Nodgaard, V. Dharmavaram, R.M. Fesinmeyer, H. Hultgen, S. Brych, R.L. Remmele, D.N. Brems, S. Hershenson, Self-buffering antibody formulations, J. Pharm. Sci. 97 (8) (2008) 3051–3066.